

Search for First-Generation Scalar Leptoquarks in $p\bar{p}$ collisions at $\sqrt{s}=1.96$ TeV

(Dated: May 13, 2005)

We report on a search for pair production of first-generation scalar leptoquarks (LQ) in $p\bar{p}$ collisions at $\sqrt{s}=1.96$ TeV using an integrated luminosity of 203 pb^{-1} collected at the Fermilab Tevatron collider by the CDF experiment. We observe no evidence for LQ production in the topologies arising from $LQ\bar{L}Q \rightarrow e\bar{q}e\bar{q}$ and $LQ\bar{L}Q \rightarrow e\nu\bar{q}$, and derive 95% C.L. upper limits on the LQ production cross section. The results are combined with those obtained from a CDF search in the topology arising from $LQ\bar{L}Q \rightarrow \nu\bar{q}\nu\bar{q}$ and 95% C.L. lower limits on the LQ mass as a function of $\beta = BR(LQ \rightarrow e\bar{q})$ are derived. The limits are 236, 205 and 145 GeV/c^2 for $\beta = 1$, $\beta = 0.5$ and $\beta = 0.1$, respectively.

PACS numbers:

The remarkable symmetry between quarks and leptons in the Standard Model (SM) suggests that some more fundamental theory may exist, which allows for new interactions between them. Such interactions are mediated by a new type of particle, the leptoquark (LQ)[1] and are predicted in many extensions of the SM e.g. grand unification, technicolor, and supersymmetry with R-parity violation[2]. A LQ carries both lepton and baryon number, is a color triplet boson with spin 0 or 1, and has fractional charge. Usually it is assumed that LQs couple to fermions of the same generation to accommodate experimental constraints on flavor changing neutral currents and helicity suppressed decays.

Previous experimental limits on LQ production are summarized in [3]. The H1 and ZEUS experiments at the $e^\pm p$ collider HERA published[4] lower limits on the mass of a first generation LQ that depend on the unknown LQ $l-q$ Yukawa coupling λ . At the LEP collider, pair production of LQs can occur in e^+e^- collisions via a virtual γ or Z boson in the s -channel and lower limits have been presented in [5]. At the Fermilab Tevatron[6–8] LQ would be predominantly pair produced through $q\bar{q}$ annihilation and gg fusion. Since the production is mediated via the strong interaction it is independent of λ , in contrast to the searches at $e-p$ machines. The coupling strength to gluons is determined by color charges of the particles, and is model-independent in the case of scalar LQs. The production of vector LQ pairs depends on additional assumptions on LQ coupling to gluons and its cross section is typically larger than the cross section for scalar LQs production. Since the acceptance for vector and scalar LQ detection is similar, limits on the vector LQ mass will be more stringent.

In this Letter, we focus on a search for first-generation scalar LQ pairs produced in $p\bar{p}$ collisions at $\sqrt{s}=1.96$ TeV. A search for scalar LQ pairs decaying into $\nu\nu q\bar{q}$, resulting in jets and missing transverse energy topology has been presented in [8]. Here we study alternative final state signatures, consisting of two electrons and two jets (LQs decaying into $eejj$) or one electron, two jets, and missing transverse energy (LQs decaying in $e\nu jj$). The

results are combined and presented as function of β , the LQ branching fraction into an electron and a quark.

CDF is a general-purpose detector built to study the physics of $p\bar{p}$ collisions at the Tevatron accelerator at Fermilab and it is described in detail in [9]. The data used in the analysis were collected during the 2002-2003 Tevatron Run II. The integrated luminosity for this data sample is $203 \pm 12.2 \text{ pb}^{-1}$. Events are selected if they pass the high E_T electron trigger, requiring one electromagnetic trigger tower to be above threshold and a set of identification cuts on the electromagnetic cluster, track and shower profile. The efficiency of the trigger combinations used in the $eejj$ and $e\nu jj$ analyses have been measured using $Z \rightarrow ee$ data[10, 11] and it is $\sim 100\%$. Electrons are reconstructed offline as calorimeter electromagnetic clusters matching a track in the central-tracking system (central electrons, $|\eta| < 1.0$ [15]) or as calorimeter electromagnetic clusters only in the forward region ($|\eta| \leq 3$). Electromagnetic clusters are identified by the characteristics of their energy deposition in the calorimeter: cuts are applied on the fraction of the energy in the electromagnetic calorimeter and the isolation of the cluster. The identification efficiency for a pair of central electrons is $\sim 92\%$ and for a pair of central-forward electrons $\sim 80\%$. The coordinate of the lepton (also assumed to be the event coordinate) along the beamline must fall within 60 cm of the center of the detector (z_{vertex} cut) to ensure a good energy measurement in the calorimeter. This cut is 95% efficient, as determined from studies with minimum bias events. The efficiencies of the identification cuts, the trigger selection and the vertex cut, measured using $Z \rightarrow ee$ data were taken into account when evaluating the signal acceptance and background estimate. Jets are reconstructed using a cone of fixed radius $R = \sqrt{(\Delta\eta)^2 + (\Delta\phi)^2} = 0.7$ and required to have $|\eta| < 2.0$. Jets have been calibrated as function of η and E_T and their energy is corrected to the parton level[12]. Neutrinos produce missing transverse energy, \cancel{E}_T , which is measured by balancing the calorimeter energy in the transverse plane.

In the analyses the we describe, the signal selection

criteria are set according to the kinematic distribution (e.g. E_T of the electrons and E_T of the jets) of decay products determined from Monte Carlo (MC) studies, optimized to eliminate background with a minimal loss of signal events[13, 14]. In the dielectron and jets topology, we select events with two reconstructed isolated electrons with $E_T > 25$ GeV from the inclusive electron triggers dataset. At least one electron is required to be central, while the other can be central or forward. Events are further selected if there are at least two jets with $E_T > 30$ and 15 GeV. The dataset selected above is dominated by QCD production of Z bosons in association with jets and $t\bar{t}$ production (where both the W 's from top decay into an electron and neutrino). To reduce these backgrounds the following cuts are applied: i) veto of events whose reconstructed dilepton mass falls in the window $76 < m_{ee} < 110$ GeV/ c^2 to remove the most of the $Z +$ jets contribution, ii) $E_T(j_1) + E_T(j_2) > 85$ GeV and $E_T(e_1) + E_T(e_2) > 85$ GeV, iii) $\sqrt{(E_T(j_1) + E_T(j_2))^2 + (E_T(e_1) + E_T(e_2))^2} > 200$ GeV to remove the remaining $Z +$ jets and top contributions. We studied the properties of the physics backgrounds by generating the process $Z + 2$ jets with Alpgen[16] + HERWIG[17] (to perform parton showering) and $t\bar{t}$ with PYTHIA[18], then passing them through a complete simulation of the CDF II detector based on GEANT[19] and full event reconstruction. Other backgrounds from $b\bar{b}$, $Z \rightarrow \tau\bar{\tau}$, WW are negligible due to the electron isolation and large electron and jet transverse energy requirements. To normalize the number of simulated events to data we used the theoretical cross sections for $t\bar{t}$ from [20] and for $\gamma/Z \rightarrow ee + 2$ jets from [21]. The expected number of $Z + 2$ jets events is 1.9 ± 0.4 . The expected number of $t\bar{t}$ events is 0.35 ± 0.06 events. The background arising from multijet events where a jet is mismeasured as an electron (fake) is calculated using data, for both this analysis and the one that follows. The method used relies on the assumption that the fake electron produced by a jet will be accompanied by other particles produced by the fragmentation of the jet; thus the isolation fraction of the fake electron will generally be larger than the one corresponding to a real electron. The isolation fraction is defined here as: $(E_T^{cone} - E_T^{cluster})/E_T^{cluster}$ where E_T^{cone} is the sum of the electromagnetic and transverse energies measured in all towers in a radius $R = \sqrt{(\Delta\phi^2 + \Delta\eta^2)}$ around the electron and $E_T^{cluster}$ is the transverse electromagnetic energy of the electron. The phase space corresponding to the two electron isolation fractions ($eejj$) or to one electron isolation fraction and the \cancel{E}_T ($evjj$) is divided in different regions. We assume that there is no correlation between the isolation of the two electrons ($eejj$) and the isolation of the electron and \cancel{E}_T ($evjj$). In the region where both electrons have large isolation fraction ($eejj$), or where the \cancel{E}_T is small and the isolation fraction of the electron is large ($evjj$) the LQ contribution is expected

TABLE I: Efficiencies after all cuts with total error (statistical and systematic) and 95% C.L. upper limits on the production cross section \times branching fraction Br, as a function of M_{LQ} , for the two channels.

M_{LQ} (GeV/ c^2)	$eejj$		$evjj$	
	ϵ	(%) $\sigma \times \text{Br}(\text{pb})$	ϵ	(%) $\sigma \times \text{Br}(\text{pb})$
100	7 ± 0.5	1.11	2 ± 0.26	5.71
140	12 ± 0.5	0.25	8 ± 0.7	0.69
160	21 ± 0.8	0.14	8 ± 0.7	0.65
200	32 ± 1.2	0.09	16 ± 1.3	0.37
220	35 ± 2.0	0.08	19 ± 1.5	0.24
240	38 ± 2.0	0.07	20 ± 1.6	0.23
260	40 ± 2.0	0.07	22 ± 1.7	0.22

to be negligible. We call these background-dominated regions. With these assumptions from the ratio of the number of events in the background-dominated regions we can extrapolate the contribution in the signal region. We estimate $0_{-0}^{+0.7}$ fake events in the central-central category and 3.96 ± 1.98 in the central-forward category. The final background estimate is 6.2 ± 2.2 events. We checked the prediction of our background sources with data in a *control* region defined by requiring two electrons with $E_T > 25$ GeV, 2 jets with $E_T > 30$ GeV and $66 < m_{ee} < 110$ GeV/ c^2 . We observe 107 events in agreement with 113 ± 15 predicted from SM processes. The efficiency to detect our signal was obtained from MC simulated LQ (PYTHIA) to account for kinematical and geometrical acceptances and it is reported in Table I for various LQ mass values. The following systematic uncertainties are considered when calculating signal acceptance and background predictions: luminosity (6%), choice of parton distribution functions (2.1%), statistical uncertainty of MC ($< 1\%$), jet energy scale ($< 1\%$), statistics of $Z \rightarrow e^+e^-$ sample (0.8%) and z_{vertex} cut (0.5%). After all selection cuts, 4 events are left in the data.

In the search in the electron and neutrino plus two jets topology, we select events with one reconstructed isolated electron with $E_T > 25$ GeV. The electron is required to be central ($|\eta| \leq 1.0$). We veto events with a second central or forward electron to be orthogonal to the previous analysis. We then select events where there is a large missing transverse energy, $\cancel{E}_T > 60$ GeV and at least two jets with $E_T > 30$ GeV in the range $|\eta| \leq 2$. This time the selected dataset is dominated by QCD production of W bosons in association with jets and top quark pairs, where either both the W 's from the top pair decay into $l\nu$ and one lepton is mismeasured, or one of the W decays leptonically and the other hadronically. A small source of background is represented by $Z + 2$ jets, where one of the electrons is not identified. To reduce these backgrounds the following cuts are applied: i) $\Delta\phi(\cancel{E}_T - jet) > 10^\circ$ to veto events where the transverse missing energy is mis-measured due to a mismeas-

sured jet, ii) $E_T(j_1) + E_T(j_2) > 80 \text{ GeV}$, iii) transverse mass of electron-neutrino system, $M_T(e\nu) > 120 \text{ GeV}/c^2$ to reduce the $W + 2$ jets contribution. We studied the properties of the $W + 2$ jets, $t\bar{t}$ and $Z + 2$ jets backgrounds using MC simulated events (AlpGen + HERWIG and PYTHIA). The background from $W \rightarrow \nu_\tau \tau + 2$ jets (AlpGen+HERWIG) is negligible after the final window mass cut (see below), as well as the QCD fakes background. Our final cut consists in selecting events falling in a mass windows defined around the LQ mass in the following way. We calculate the invariant mass of the electron-jet system and the transverse mass of the neutrino-jet system. Given the decay of the two LQs, there are two possible mass combinations for the electron and the neutrino with the two leading jets. We choose the combinations that minimize the difference between the electron-jet mass and the neutrino-jet transverse mass. We fit the peak of the e -jet distribution with a Gaussian, to obtain an estimate of the spread of the distribution in the signal region (σ_e), as well as the ν - jet transverse mass distribution, to obtain σ_ν . In the kinematic plane of $m(e - jet)$ vs $m_T(\nu - jet)$ we define the sides of rectangular boxes centered around various nominal LQ mass as $3 \times \sigma_{e,\nu}$. For each LQ mass, events are accepted if they fall inside the rectangular box. The overall selection efficiency for various LQ masses is given in Table I. We checked the simulation prediction of our background sources with data in a *control* region defined by requiring one electron with $E_T > 25 \text{ GeV}$, $\cancel{E}_T > 35 \text{ GeV}$ and 2 jets with $E_T > 30 \text{ GeV}$. We observe 536 events in agreement with 503 ± 22 predicted from SM processes. The efficiency to detect our signal was obtained from MC simulated LQ data (PYTHIA). The following systematic uncertainties are considered when calculating signal acceptance and background predictions: luminosity (6%), choice of the parton distribution functions (2.1%), statistics of MC ($< 1.0\%$), jet energy scale ($< 1\%$), electron identification (0.6%), z_{vertex} cut (0.5%), initial and final state radiation (1.7%). The number of events in each mass region, after all selection cuts, compared with the background expectations is reported in Table II.

In the analyses described above the number of events passing the selection cuts is consistent with the expected number of background events. The conclusion of the two searches is that there is no LQ signal: hence we derive an upper limit on the LQ production cross section at 95% confidence level. We use a Bayesian approach[22] with a flat prior for the signal cross section and Gaussian priors for acceptance and background uncertainties. The cross section limits are tabulated in Table I and the mass limits are tabulated in Table III. To compare our experimental results with the theoretical expectation, we use the next-to-leading order (NLO) cross-section for scalar LQ pair production from Ref.[23] with CTEQ4 PDF[24]. The theoretical uncertainties correspond to the variations from $M_{LQ}/2$ to $2M_{LQ}$ of the renormalization scale μ used in

TABLE II: Final number of events surviving all cuts in the electron, missing energy and jets topology, compared with background expectations, as function of the LQ mass (in GeV/c^2). Errors include statistical and systematic uncertainty.

Mass	W + 2 jets	top	Z + 2 jets	Total	Data
120	1.5 ± 0.9	3.3 ± 0.5	0.06 ± 0.01	4.9 ± 1.0	6
140	1.5 ± 0.9	3.1 ± 0.6	0.08 ± 0.02	4.7 ± 1.0	4
160	2.5 ± 1.1	2.8 ± 0.6	0.08 ± 0.02	5.4 ± 1.2	4
180	2.5 ± 1.1	2.4 ± 0.5	0.08 ± 0.02	5.0 ± 1.2	4
200	2.5 ± 1.1	2.0 ± 0.5	0.07 ± 0.02	4.6 ± 1.2	4
220	2.0 ± 1.0	1.6 ± 0.3	0.06 ± 0.02	3.7 ± 1.1	2
240	2.0 ± 1.0	1.1 ± 0.3	0.06 ± 0.02	3.1 ± 1.0	2
260	1.5 ± 1.0	0.8 ± 0.3	0.04 ± 0.02	2.4 ± 0.9	2

the calculation. To set a limit on the LQ mass we compare our 95% CL upper experimental limit to the theoretical cross section for $\mu = 2M_{LQ}$, which is conservative as it corresponds to the lower value of the theoretical cross section. We find lower limits on $M(LQ)$ at $235 \text{ GeV}/c^2$ ($\beta = 1$) and $176 \text{ GeV}/c^2$ ($\beta = 0.5$). To obtain the best limit, we have combined the results from the two decay channels just described with the result of a search for LQ in the case where the LQ pair decays to neutrino and quark with branching ratio $Br(LQ \rightarrow \nu q) = 1.0 = 1 - \beta$ [8]. The individual channels analyses are in fact optimized for fixed values of β (1,0.5,0) while in the combined analysis, due to the contributions of the different decay channels, the signal acceptance can be naturally be expressed as a function of β . As for the treatment of uncertainties, the searches in the $eejj$ and $e\nu jj$ channel use common criteria and sometimes apply the same kind of requirements so the uncertainties in the acceptances have been considered correlated. When calculating the limit combination including the $\nu\nu jj$ channel the uncertainties have been considered uncorrelated. For each β value a 95% C.L. upper limit on the expected number of events is returned for each mass, and by comparing this to the theoretical expectation, lower limits on the LQ mass are set. The combined limit as a function of β is shown in Figure 1, together with the individual channel limits. The combined mass limits are also tabulated in Table III.

In conclusion, we have performed a search for pair production of first generation scalar LQs using 203 pb^{-1} of proton-antiproton collision data recorded by the CDF experiment during Run II of the Tevatron. The results from all the final state signatures are combined and no evidence of LQs production is observed. Assuming that a scalar LQ decays to electron and quark with variable branching ratio β we exclude LQs with masses below $236 \text{ GeV}/c^2$ for $\beta = 1$, $205 \text{ GeV}/c^2$ for $\beta = 0.5$ and $145 \text{ GeV}/c^2$ for $\beta = 0.1$.

We thank the Fermilab staff and the technical staffs of the participating institutions for their vital contributions.

TABLE III: 95% C.L. lower limits on the first generation scalar LQ mass (in GeV/c^2), as a function of β . The limit from CDF[7] ($eejj$) Run I ($\sim 120\text{pb}^{-1}$) is also given.

β	ee jj	$evjj$	$\nu\nu jj$	Combined	CDF Run I
0.01	< 100	< 100	116	126	-
0.05	< 100	< 100	112	134	-
0.1	< 100	144	< 80	145	-
0.2	< 100	158	< 80	163	-
0.3	114	167	< 80	180	-
0.4	165	174	< 80	193	-
0.5	183	176	< 80	205	-
0.6	197	174	< 80	215	-
0.7	207	167	< 80	222	-
0.8	216	158	< 80	227	-
0.9	226	144	< 80	231	-
1.0	235	<100	< 80	236	213

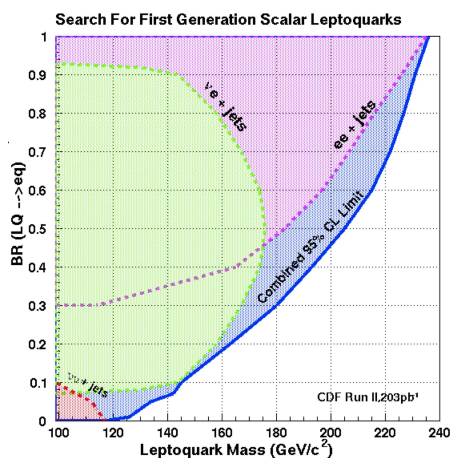


FIG. 1: LQ mass exclusion regions at 95% C.L. as function of $\text{Br}(\text{LQ} \rightarrow \text{eq})$.

This work was supported by the U.S. Department of Energy and National Science Foundation; the Italian Istituto Nazionale di Fisica Nucleare; the Ministry of Education, Culture, Sports, Science and Technology of Japan; the Natural Sciences and Engineering Research Council of Canada; the National Science Council of the Republic of China; the Swiss National Science Foundation; the A.P. Sloan Foundation; the Bundesministerium fuer Bildung und Forschung, Germany; the Korean Science and Engineering Foundation and the Korean Research Foundation; the Particle Physics and Astronomy Research Council and the Royal Society, UK; the Russian Foundation for Basic Research; the Comisi3n Interministerial de Ciencia y Tecnolog3a, Spain; and in part by the European Community's Human Potential Programme under contract HPRN-CT-20002, Probe for New Physics.

- [2] D.Acosta and S.K. Blessing, *Ann.Rev.Nucl. Part.Sci.* **49**, 389 (1999) and reference therein.
- [3] G.Moortgat-Pick, S.Rolli, A.F.Zarnecki, *Acta Phys. Polon.*B33:3955-3981, 2002.
- [4] H1 Collaboration, C, Adloff et al., *Eur. Phys. J.C* **11**, 447 (1999); Erratum *ibid. C* **14** 553 (2000); H1 Collaboration, C, Adloff et al., *Phys.Lett. B* **523**, 234 (2001); ZEUS Collaboration, J. Breitweg et al., *Eur. Phys. J.C* **16**, 253 (2000); ZEUS Collaboration, J. Breitweg et al., *Phys.Rev.D* **63**, 052002 (2001).
- [5] DELPHI Collaboration, P. Abreu et al., *Phys. Lett. B* **446** 62 (1999); L3 Collaboration, M. Acciari et al., *Phys. Lett. B* **489** 81 (2000); ALEPH Collaboration, R. Barate et al.,*Eur. Phys. J.C* **12**, 183 (2000); OPAL Collaboration, G. Abbiendi et al., *Phys. Lett. B* **526** 233 (2002).
- [6] D0 Collaboration, V. Abazov et al.,*Phys. Rev. D* **64**, 092004 (2001); D0 Collaboration, hep-ex/0412029; Fermilab-Pub-04/389-E, Dec 2004.
- [7] CDF Collaboration, F. Abe et al.,*Phys. Rev. Lett.* **79**, 4327 (1997).
- [8] CDF Collaboration, D. Acosta et al., hep-ph/0410076, submitted to PRL.
- [9] CDF Collaboration, D. Acosta et al., *Phys. Rev. D* **71**, 032001 (2005).
- [10] CDF Collaboration, D. Acosta et al., *Phys.Rev.Lett.*94:091803,2005
- [11] M.Karagoz-Unel, Proceeding of HCP2004, hep-ex/0411067
- [12] CDF Collaboration, D. Acosta et al. *Phys. Rev. Lett.* **74**, 2626 (1995).
- [13] D. Ryan, Ph.D. Thesis, Tufts University, 2004.
- [14] F. Strumia-Michelini, Ph.D. Thesis, University of Geneva, 2000.
- [15] We use a cylindrical coordinate system around the beampipe in which θ is the polar angle, ϕ is the azimuthal angle and $\eta = -\ln(\tan(\frac{\theta}{2}))$. $E_T = E \sin \theta$ and $P_T = P \sin \theta$, where E is the energy measured by the calorimeter and P the momentum measured by the tracking system. $\vec{E}_T = -\sum E_T^i \vec{n}_i$ where \vec{n}_i is a unit vector that points from the interaction vertex to the i th calorimeter tower in the transverse plane. E_T is the magnitude of \vec{E}_T . \vec{E}_T is corrected following the correction of jet energies, and if muons are identified in the event, \vec{E}_T is corrected for the muon momenta.
- [16] M.L.Mangano et al., *JHEP* **0307**,001 (2003).
- [17] G. Corcella et al., *JHEP* **01**, 10 (2001).
- [18] T. Sjostrand et al., *Comput. Phys. Commun.* **135**, 238 (2001).
- [19] R. Brun and F. Carminati, CERN Program Library Long Writup W5013 (1993).
- [20] N.Kidonakis and R. Vogt, *Phys.Rev.D* **68**, 114014 (2003) M.Cacciari et al., *JHEP* **404**, 68 (2004).
- [21] J. Campbell, R.K. Ellis, *Phys. Rev. D* **65**:113007 (2002).
- [22] J.Conway, CERN 2000-005, 247 (2000). The posterior probability density is rendered normalizable by introducing a reasonably large cutoff.
- [23] M. Kramer et al., *Phys Rev Lett* **79**, 341, 1997.
- [24] J. Pumplin et al., *JHEP* **0207** (2002) 012.

[1] W. Buchmuller, R. Ruckl and D. Wyler, *Phys. Lett.* B191, 442 (1987) and Erratum B448, 320 (1999).